Chapter 4
Metal Nanoparticles: Synthesis, Characterization, and Biomedical Applications

Sivasankar Putta, Raj Kumar Sharma, and Puneet Khandelwal

Abstract Metallic nanoparticles have attracted the attention of researchers worldwide because of their fascinating optical, electrical, magnetic, and catalytic properties. Metallic nanoparticles have an easy surface modification chemistry to attach various molecules such as ligands, targeting agents, biomolecules, drugs, and antibodies. Because of the different properties and easy modification chemistry, these nanoparticles have wide-ranging applications, including biomedical, solar, catalysis, etc. This chapter will focus on metallic nanoparticles, specifically gold nanoparticles, for biomedical applications.

Keywords Metal nanoparticles · Gold nanoparticles · Nanomedicine · Gene silencing · Phototherapy · Immunotherapy · CRISPR–Cas9 · Radiotherapy

4.1 Introduction

Metals have been a center of attraction over the last two centuries because of their fascinating physical and biological properties. A PubMed search shows the presence of around 1.5 million research documents on metals since 1800. The metals in their nano form, known as bhasma, have been used in India since ancient times to treat various diseases. However, the concept of nanotechnology was introduced in the last century (1959) by physics Nobel laureate Richard P. Feynman in his famous lecture titled "There's Plenty of Room at the Bottom" at the meeting of the American Physical Society [1, 2]. The terminology "nanotechnology" was introduced by Norio Taniguchi in 1974.

Gold nanoparticles have unique physical, chemical, and optical properties, which leads to their excellent biocompatibility, easy synthesis in a broad range of sizes

S. Putta
Department of Chemistry and Biochemistry, University of California, Santa Cruz, CA 95064, USA

R. K. Sharma · P. Khandelwal (✉)
Department of Radiology, School of Medicine, Johns Hopkins University, Baltimore, MD 21202, USA
e-mail: pkhande3@jhmi.edu

D. K. Singh et al. (eds.), *Nanomaterials*,
https://doi.org/10.1007/978-981-19-7963-7_4

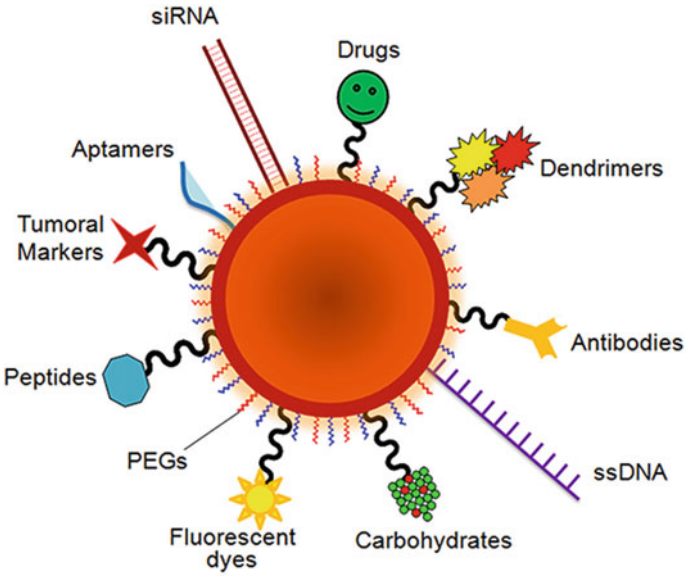

Fig. 4.1 Various biomolecules can be attached to the gold nanoparticle's surface, providing enhanced biocompatibility, chemical stability, functionality, and specificity for targeted therapy and imaging applications. Adapted with permission from Ref. [3] (Copyright 2014 Frontiers Media)

and shapes in an aqueous medium, easy surface functionalization, and photostability, and photo-thermal activity (Fig. 4.1) [3]. Due to their strong optical properties originating from the localized surface plasmon resonance and their high surface-to-volume ratio, these nanoparticles have been used for efficient light-to-heat conversion (photo-thermal therapy), sensors (sensing biomolecules and heavy metal ions), and imaging applications [4]. In 1857, Faraday described the synthesis of colloidal gold nanoparticles for the first time by reducing gold chloride ($AuCl^{4-}$) using phosphorus and their stabilization by carbon disulfide. Later, Turkevich et al. reported the colloidal gold nanoparticle synthesis by trisodium citrate to reduce gold chloride in the aqueous medium [5, 6].

4.2 Synthesis of Metal Nanoparticles

The metal nanoparticles can be synthesized by two main methods: (1) The top-down approach and (2) the bottom-up approach. Both of these methods differ mainly by starting material. In the top-down process, the starting material is bulk, the size of which is reduced to nano dimension by various physical, chemical, or mechanical methods. On the other hand, the bottom-up approach uses atoms and molecules as the starting materials [7]. The synthesis of nanoparticles is based on the decrease in the size of the initial material by different physical, chemical, and biological treatments.

Although the top-down approach is easy to operate, it is not appropriate for preparing informally shaped and microscopic particles. The major challenge with this method is the change in surface chemistry and physicochemical properties of synthesized nanoparticles [8, 9].

The bottom-up approach is based on the formation of nanoparticles from smaller molecules and/or atoms, including joining atoms, molecules, or small particles. In this process, the nanostructured building blocks are first synthesized, followed by their assembly to synthesize the final nanoparticles [10–13].

Mechanical milling method

Mechanical milling is a kind of grinding method which uses high-speed rotating balls to reduce the particle size of the bulk material. The bulk material is introduced into a rolling hollow cylinder with high-speed rotating balls dropping from the top of the cylinder to the bulk material, reducing particle size. This method is environment-friendly and cost-effective; therefore, it has wide applications in industries.

Laser ablation method

Laser ablation, also known as the photoablation method, is used to make nanoparticles from bulk material. The bulk material is irradiated with a pulse laser such as Nd:YAG, Ti:Sapphire, and copper vapor laser, resulting in nanoparticle suspension. The time duration, wavelength, and fluency of the laser and surrounding medium affect the synthesized nanoparticles. The laser ablation method is suitable for making homogenous and monodisperse nanoparticles with a high production rate.

Physical vapor deposition method

In this method, the metal vapor is deposited on an electrically conductive material either as a thin film or as nanoparticles. The ion beam sputtering method uses inert gas ions (such as argon) to make the plasma surrounding the target material. The argon ions then strike the target material (at high voltage), which will eject the atoms from the target material and deposit them onto the substrate. The entire process is performed at a very high pressure of about 10^{-1} to 10^{-3} mbar. Magnetron sputtering has been used successfully to synthesize various nanoparticles [14].

Chemical vapor deposition method

Unlike the physical vapor method, the chemical vapor deposition approach involves the reaction of chemical vapors containing more volatile precursors with the target material. The thin film of the target material is deposited on a substrate [15]. This approach is widely used in semiconductors to make thin films.

Sol–gel method

The sol–gel nanoparticle synthesis method involves the synthesis of metal alkoxide precursors in solution (sol phase), which further acts as a building block for an integrated metal oxide network (gel phase) [16]. This method is generally used for the synthesis of metal oxide nanoparticles.

Chemical reduction method

The metal salt is reduced in an aqueous medium using different chemical reducing agents in the presence of a surfactant. Examples of reducing agents are sodium borohydride, sodium citrate, and ascorbic acid. Formed metal nanoparticles are capped with stabilizing or capping agents such as long-chain alkylates and long-chain fatty acids, including sodium lauryl sulfate and hexadecyltrimethylammonium bromide. Sometimes, a stabilizing agent can also act as a reducing agent, such as sodium citrate and ascorbic acid. Many biomolecules containing amine, oxide, or thiol groups may act as reducing and capping agents [17–20]. This is one of the most popular methods for synthesizing metal nanoparticles.

Hydrothermal method

The hydrothermal approach to synthesizing nanoparticles involves the growth of a single crystal in high vapor pressure and high-temperature environment. This environment is created in specially designed thick-walled vessels of high corrosion and temperature-resistant steel [21–27].

Solvothermal method

The solvothermal method is similar to the hydrothermal method in most ways which also uses a high-temperature and high-pressure environment developed inside a thick-walled steel vessel. The significant difference in both approaches is that the latter uses organic solvents instead of aqueous solvents [28].

Pyrolysis

Pyrolysis is the process of chemical transformation or decomposition of material in an inert atmosphere at a high temperature. The spray pyrolysis approach involves the delivery of nanoparticle precursors in vapor form using a nebulizer into the hot reactor. On the other hand, the laser pyrolysis method involves the precursors absorbing laser energy for the preparation of nanoparticles. In the flame pyrolysis approach, the liquid precursors are directly sprayed into the flame [29].

Biological method

The biological method is a cost-effective, eco-friendly, green synthesis approach involving the use of different microorganisms and plant products for nanoparticle synthesis. The biological process has an advantage over other methods because this method doesn't require high temperature, pressure, and toxic chemicals [30].

Electrochemical deposition

The electrochemical method is a process in which a thin metal layer has been deposited on the conducting material surface. The metal precursor ions get reduced at the conducting surface and make a thin layer of metal coating in the presence of sufficient electric current [31].

Microwave-assisted synthesis

Microwave-assisted synthesis is preferred over the thermal approach because of its fast, homogenous heating and high product yield. Microwave frequency of 300 MHz to 300 GHz leads to the polar molecule orientation with the electric field. In contrast, re-orientation with an alternating electric field triggers molecular friction and energy loss in the form of heat [32–34].

Ultrasound-assisted synthesis

The ultrasound approach uses the cavitation process, which is the formation and collapse of the bubble by intense ultrasound waves, producing an enormous amount of kinetic energy which converts into heat. This process has an advantage over other conventional methods in that it produces a high yield, requires low energy, doesn't need toxic chemicals, and produces low waste [35].

4.3 Characterization of Metal Nanoparticles

Several technologies have been used to characterize the physical, chemical, and optical properties of nanoparticles, such as shape, size, crystal structure, elemental composition, and stability.

4.3.1 Spectroscopic Characterization

The metallic nanoparticles show characteristic optical properties due to the oscillations of the conduction band of electrons at the surface of nanoparticles, known as surface plasmon resonance. The color of gold nanoparticle suspension changes from deep red to purple depending on the size of the nanoparticles. Due to LSPR, some portion of the electromagnetic spectrum is absorbed while others get reflected, leading to their visible colors. The absorption of the electromagnetic spectrum can be detected in UV–Vis spectrophotometer as a strong peak between 520 and 800 nm depending upon the size of nanoparticles.

4.3.2 SEM Analysis

Scanning electron microscopy is used to characterize nanoparticle size, shape, and agglomeration. In SEM imaging, a focused electron beam is allowed to react with the sample, which produces many signals required to obtain the shape and composition of the nanoparticles. The sample processing for SEM is very straightforward in that

the sample must be drop-casted on the conductive substrate and dried thoroughly to remove any solvent traces.

4.3.3 TEM Analysis

Transmission electron microscopy is used to characterize the structural properties of nanoparticles. TEM can be used to produce the images, diffraction patterns, and microanalytical data of the nanomaterial to get a complete insight into the different properties and behavior of nanomaterials. Unlike SEM, TEM sample preparation includes a diluted sample drop cast on the carbon-coated copper grid.

4.3.4 AFM Analysis

The atomic force microscope uses phosphorus-doped silicon probes, which scan the entire nanoparticle surface and provide 3D projection images of nanoparticles. AFM can also give extensive qualitative and quantitative data depending on the type of nanomaterial. The sample preparation for AFM is very similar to the SEM.

4.3.5 FTIR Analysis

The Fourier transform infrared (FTIR) spectroscopy utilizes infrared waves to analyze the chemical structure of the nanomaterial at the molecular scale, especially the bonding of capping agents to the nanoparticle surface. The sample preparation includes mixing and grinding of completely dried nanomaterial with KBr powder.

4.3.6 XRD Analysis

X-ray diffraction utilizes the constructive interference between X-ray radiation and the nanomaterials, which generates information about the structure of nanomaterials, especially the crystal structure, crystallite size, nature of phase, lattice parameters, and strain.

4.4 Metal Nanoparticles for Biomedical Applications

4.4.1 Chemotherapy

The ease of surface functionalization of gold nanoparticles through various biomolecules made them an attractive delivery agent for chemotherapy. There are different methods developed for the functionalization of gold nanoparticles. In one method, prodrugs can be coupled covalently to the gold nanoparticles via cleavable linkers [36–39]. In another approach, hydrophobic drug molecules can be non-covalently attached to gold nanoparticles, allowing delivery without any structural change of the drug molecules [10–13]. Gold nanoparticles can release the drugs by either internal (e.g., glutathione) or external (e.g., light) stimuli [40–46]. The diversity of the gold nanoparticle monolayer is crucial to both release mechanisms, offering tunability for endogenous delivery processes and a functional platform for external delivery approaches [47].

4.4.2 Phototherapy

Sunlight has been used in medicine from ancient Egypt, Greece, India, and China to treat various diseases [48]. The disorders such as psoriasis and vitiligo were treated using vegetal-derived substances in the presence of sunlight in ancient Egypt [49]. In ancient times, light therapies had also been used to treat several other disorders, such as physiological illnesses, sleep, skin diseases, neonatal jaundice, retinal correction, and cancer.

However, the use of light irradiation has recently been shown for the precision therapy of cancer treatment. The light can be used directly to initiate physiological changes or endogenous biochemical reactions, which leads to cell damage [50]. The light can also be used indirectly to initiate the production of effector molecules as byproducts [49, 51, 52]. According to the method, the use of light can be broadly divided into two different categories: (a) Photodynamic therapy—in this method, sensitizer molecules absorb the light and initiate a chemical alteration reaction that leads to the therapeutic outcome, and (b) Photo-thermal therapy—in this method, gold nanoparticles have been used which convert the light to heat and damage the cells (Fig. 4.2) [49, 51–55].

Phototherapy uses lasers as a light source that generates monochromatic light and can be transported through an optical fiber. The light source selection depends on the absorption of photosensitizers, location of the disease, lesion size, exposure time, total light dose, and light delivery type. The wavelength of phototherapy is chosen in the range 600–800 nm, the NIR region known as the therapeutic window. In this range of wavelength, photosensitizer molecules get excited. The significant advantage of

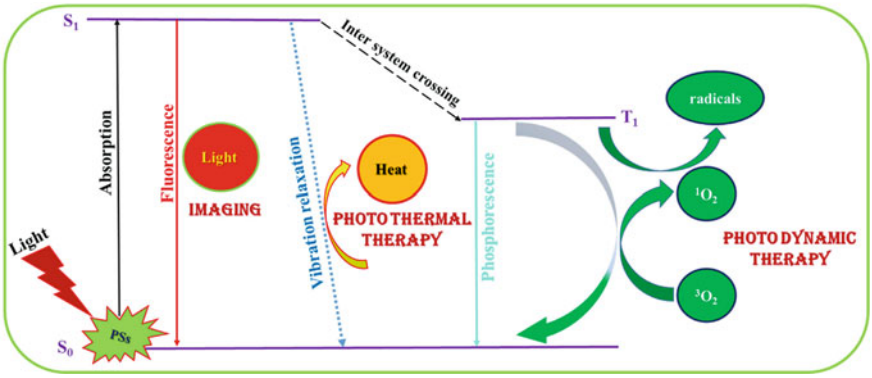

Fig. 4.2 Light-induced therapy—**a** photodynamic (PDT) and **b** photo-thermal (PTT) treatment. Schematic representation of the crucial steps of PDT and PTT used as a therapeutic approach against cancer. Adapted with permission from Ref. [50] (Copyright 2021 MDPI)

phototherapy is minimal invasiveness, tumor specificity, reduced systemic cytotoxicity, and spatiotemporally controlled illumination via focused irradiation only at the diseased lesion [56].

Gold nanoparticles have been used effectively to deliver photosensitizer molecules benefitting from the easy surface modifications of the nanoparticles. Gold nanoparticles can efficiently deliver different biomolecules, such as proteins, DNA, and drug molecules, which may act as sensitizers. The gold nanoparticles and photosensitizer conjugates can effectively transfer the energy or electrons between sensitizer and nanoparticles, making them suitable for effective PDT [51, 54, 57, 58].

Photo-thermal therapy is another minimally invasive alternative to photodynamic therapy, which utilizes the generation of controlled local heat with extreme precision. Since the early 1900s, it has been very well-known that cancer cells are more susceptible to heat than normal cells. Photo-thermal therapy utilizes photo-thermal agents and generates heat to raise the local temp as high as 40–45 °C, which is higher than the physiological temperature (36–37 °C). The photo-thermal therapy kills cancer cells by affecting several cellular and molecular mechanisms such as direct cell membrane damage, inhibition of DNA synthesis, and cytoskeleton damage. Hyperthermia therapy is not free from side effects. Hyperthermia can cause side effects because of the disproportionate photo-thermal agent's distribution throughout the body and extreme laser power [56, 59].

4.4.3 Immunotherapy

Vaccination is a kind of immunotherapy that utilizes adjuvant molecules to make the response highly efficient [60]. The development of vaccines is crucial, including the long-lasting induction of robust immune response, antigen-specific CD8+ T cell, and

stimulating antibody response to existing tumors [61]. The critical factor in developing vaccines is the delivery of antigens to antigen-presenting cells with subsequent activation and maturation. This will, in response, maximize cross-presentation for inducing cytotoxic CD8+ T cell response [62]. For this purpose, the vaccine delivery to the lymph node can be one of the best strategies because lymph nodes contain many APCs and immune cells responsible for both humoral and cellular immunity [61, 63–66].

Nanoparticles have evolved as a potential candidate for antigen delivery because they can easily be targeted to the lymph node via a lymphatic vessel in a size-dependent manner [61, 63]. Small particles around 25 nm have higher accumulations in lymph nodes than the larger ones with a size equal to or more than 100 nm [67]. Therefore, there are some critical considerations for developing nanoparticles for antigen delivery, such as (a) the nanoparticles should be smaller than 50 nm, (b) the antigen or adjuvant should be versatile to be functionalized on the nanoparticle surface, (c) the antigen should effectively activate antigen-presenting cells to induce humoral and cellular immunity, and (d) nanoparticles should be trackable non-invasively throughout the body. Given these considerations, gold nanoparticles can fit the best because of the following properties: (a) easy to control the size of gold nanoparticles from 1 nm to hundreds of nanometers, (b) various biomolecules, including protein, peptide, and oligonucleotides, can be easily attached to the gold nanoparticles surface, (c) gold nanoparticles are biocompatible, biologically inert, and non-toxic, (d) gold nanoparticles can easily be tracked throughout the body using imaging techniques such as computed tomography which is readily available in most of the hospitals or clinical centers.

Lee et al. prepared a vaccine based on gold nanoparticles (size = 7 nm) for targeted delivery to lymph nodes (Fig. 4.3). The gold nanoparticles were functionalized by red fluorescence protein (which works as an antigen), and thiol-modified CpG 1668 oligodeoxynucleotide (ODN; CpG 1668 is an ODN that contains CpG motifs, which works as a potent stimulator of the immune response). The red fluorescence protein was modified to have two cysteines at its c-terminus, which enables its coupling to the surface of gold nanoparticles via Au–S bonding [68]. The CpG 1668 with a spacer consisting of ten adenine nucleotides (A10) can effectively trigger immune responses through the activation of toll-like receptor 9 (TLR-9) [69].

Ahn et al. used the extra domain B (EDB) of fibronectin for the vaccine formulation. EDB is a tumor-associated self-antigen overexpressed in fetal and tumor tissues and is therefore known as an oncofetal antigen [70]. Moreover, EDB is also an excellent angiogenesis marker as it accumulates explicitly in the basement membrane of the neovascular structures present in aggressive tumors. AuNP/EDB-$OVA_{257–269}$ efficiently facilitated cross-presentation of the antigen in professional dendritic cells, eventually stimulating antigen-specific cytotoxic T-lymphocyte reactions. Following administration of AuNP/EDB-$OVA_{257–269}$, the vaccine efficiently reached the local lymph nodes, causing a high-level EDB-specific antibody production and finally preventing tumor growth in an EDB-overexpressing breast tumor model [70].

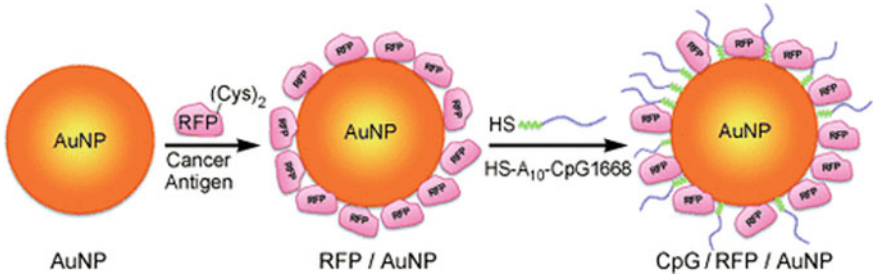

Fig. 4.3 Schematic representation of CpG/RFP/AuNPs preparation. Adapted with permission from Ref. [68] (Copyright 2014 Elsevier)

4.4.4 Radiotherapy

Due to its high-level tissue penetration, radiotherapy is one of the most extensively used non-surgical therapies for cancer patients in clinics. Various metals with high atomic numbers, such as gold, bismuth, gadolinium, and hafnium, have been widely explored as radiosensitizers. Gold has been extensively studied among these metals because of its intrinsic radiosensitivity property (due to its higher atomic number) and biocompatibility compared to other high atomic number materials [71, 72].

However, high-energy radiation, like X-rays, can damage genetic material. Therefore, delivery agents (radiosensitizers) are needed that can interact with X-rays to confine the radiation dosage into desired cells/tissues. Nanoparticles have the advantage over traditional molecular radiosensitizers because nanoparticles can be tailored to facilitate selective delivery into tumor tissues due to the enhanced permeability and retention (EPR) effect [71, 73–79].

Gold nanoparticles can be selectively delivered to the tumors, leading to higher absorption of X-rays into the tumors than in normal tissues. As per the calculations, this dose enhancement can be considerably more significant than normal tissues, even 200% or higher [71, 76]. Additional advantages of Au NPs are that they can be used as contrast for image-guided therapy and are appropriate for combinatorial therapy to deliver more than one drug molecule.

Ding et al. reported gold nanoparticles conjugated with a responsive peptide (Tat-R-EK) [80]. This responsive peptide consists of three main components: a cell and nuclear-penetrating component derived from human immunodeficiency virus-1 transactivator of transcription protein (Tat), a cathepsin B cleavable linker, and a zwitterionic antifouling component (Fig. 4.4). The peptide covered the gold nanoparticles via the Au–S bonding between gold and thiol groups from cysteine.

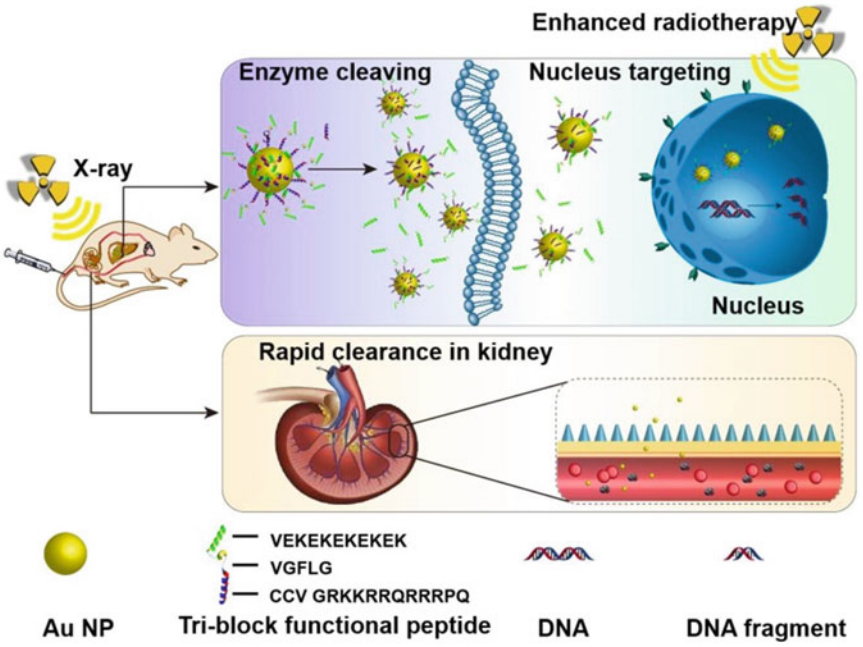

Fig. 4.4 Schematic shows the gold nanoparticle delivery in tumor tissues and cell nuclei for improved radiotherapy in vivo and fast clearance via the kidney. Adapted with permission from Ref. [80] (Copyright 2020 Ivyspring International Publisher)

4.4.5 Gene Silencing

4.4.5.1 RNAi

The gold nanoparticles have been extensively studied to deliver siRNA for gene knockdown purposes. There are two ways to attach the siRNA with gold nanoparticles: (a) via Au–S chemistry or (b) via electrostatic interactions.

Au–S bonding has been used to bind thiol-containing ligands to the surface of gold nanoparticles. In a study by Giljohann et al., 13 nm gold nanoparticles were co-loaded with SH–PEG400 and SH–siRNA (Fig. 4.5). In this system, the PEG was significantly smaller than the siRNA, so the nanoparticle surface displayed to the cells exhibits almost entirely siRNA [81].

Electrostatic interactions have also been used for attaching the negatively charged siRNA molecules to the surface of gold nanoparticles via positively charged polymers such as polyethyleneimine (Fig. 4.6). For example, Elbakry et al. reported a complex with a 15 nm gold nanoparticle core followed by layers of PEI, siRNA, and PEI [82].

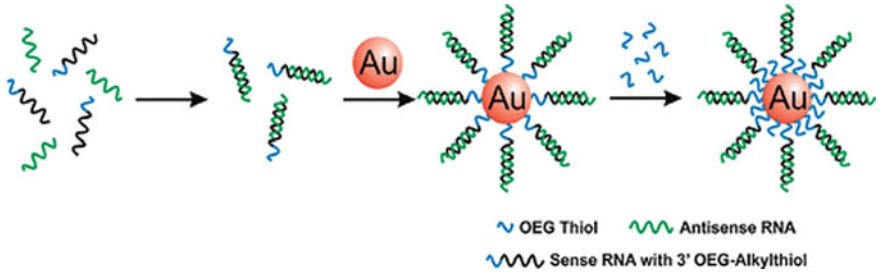

Fig. 4.5 Preparation of siRNA conjugated gold nanoparticles. The RNA duplex was formed first, followed by the addition of gold nanoparticles and OEG-alkylthiol. Adapted with permission from Ref. [81]. Copyrights 2009 American Chemical Society

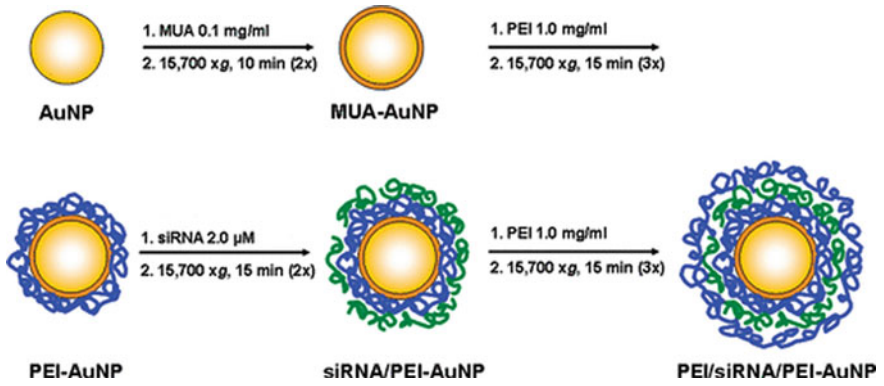

Fig. 4.6 Flowchart illustrating the layer-by-layer deposition applied to gold nanoparticles. After each coating step, gold nanoparticles were purified by centrifugation and resuspended in unbuffered 10 mM NaCl. Adapted with permission from Ref. [82]. Copyrights 2009 American Chemical Society

4.4.5.2 CRISPR–Cas9

The discovery and translation of clustered regularly interspaced short palindromic repeats (CRISPR)/Cas9 from bacteria to mammalian cells demonstrated a milestone for genome engineering due to its robustness, simplicity, and versatility [83–85]. There are two main types of gene-editing therapies that have been used for the CRISPR–Cas9 system: (1) non-homologous end joining (NHEJ), which completely silences disease-producing genes by introducing indel mutations, and (2) homology-directed repair (HDR), which reverts disease-producing gene mutations to their wild-type form. HDR-based therapies can treat most genetic diseases. Therefore, there is considerable interest in advancing HDR-based therapeutics. However, in vivo gene editing via HDR is difficult due to the targeted delivery of Cas9, guide RNA (gRNA), and donor DNA [86–90].

Gene therapy using adeno-associated viruses (AAVs) is presently the highly developed and used approach for delivering Cas9 in vivo. However, in vivo AAV delivery is difficult because a substantial portion of the human population has pre-existing immunity toward AAV, making them disqualified for therapeutics [91]. Moreover, the AAV-based Cas9-delivery system also generates considerable off-target genomic modifications because of the constant expression of Cas9. AAV also has a smaller packing size and may need several viruses to deliver Cas9 ribonucleoprotein (RNP) and donor DNA in vivo, which may reduce the HDR efficiency of the AAV-based Cas9-delivery system. Finally, the viral titers required to produce curative amounts of editing have been way higher than the clinically accepted levels [92–96]. Therefore, the reliable and effective delivery of CRISPR/Cas9 remains a significant challenge restricting its wide applications. For this reason, gold nanoparticles have been explored for efficient delivery [91, 97–100].

Lee et al. developed "CRISPR–Gold," which can deliver Cas9 RNP and donor DNA in vivo and stimulate HDR [90]. CRISPR–Gold is composed of gold nanoparticles coupled with DNA, which are complexed with donor DNA, Cas9 RNP, and poly(N-(N-(2-aminoethyl)-2-aminoethyl) aspartamide) (PAsp(DET)) which is an endosomal-disruptive polymer. CRISPR–Gold is created to be internalized by cells via endocytosis due to the cationic PAsp(DET), which complexes with the components of CRISPR–Gold (Fig. 4.7). After endocytosis, the cationic polymer on CRISPR–Gold activates endosomal disruption and triggers the delivery of CRISPR–Gold into the cytoplasm. Importantly, once in the cytoplasm, glutathione releases the DNA from the gold core of CRISPR–Gold, which causes the rapid release of Cas9 RNP and donor DNA.

CRISPR–Gold was capable of targeting CXCR4 in human embryonic stem cells, human-induced pluripotent stem cells, bone-marrow-derived dendritic cells, and the dystrophin gene in myoblasts with an HDR efficiency between 3 and 4%. CRISPR–Gold can also deliver Cas9 RNP and generate gene deletions in Ai9 mice. CRISPR–Gold was capable of correcting the mutated dystrophin gene in mdx mice to the wild-type sequence after a single dose and restoring dystrophin protein expression in muscle tissue. CRISPR–Gold can stimulate HDR in the dystrophin gene. In particular, 5.4% of the dystrophin gene in mdx mice was corrected back to the wild-type after CRISPR–Gold therapy. This correction rate was around 18 times higher than treatment with Cas9 RNP and donor DNA alone, with only a 0.3% correction rate.

Wang et al. used lipids such as DOTAP, DOPE, cholesterol, and PEG2000-DSPE to coat TAT-modified gold nanoparticles to deliver the Cas9-sgPlk-1 plasmid [101]. The lipids can facilitate the entry of gold nanoparticles into the cells, while TAT peptides can take the plasmid into the nucleus. A laser-triggered thermal effect caused the release of plasmid from nanoparticles. On day 20, the tumor volume decreased to about 42% with the nanoparticles and 20% with the nanoparticles and laser irradiation compared to the control group.

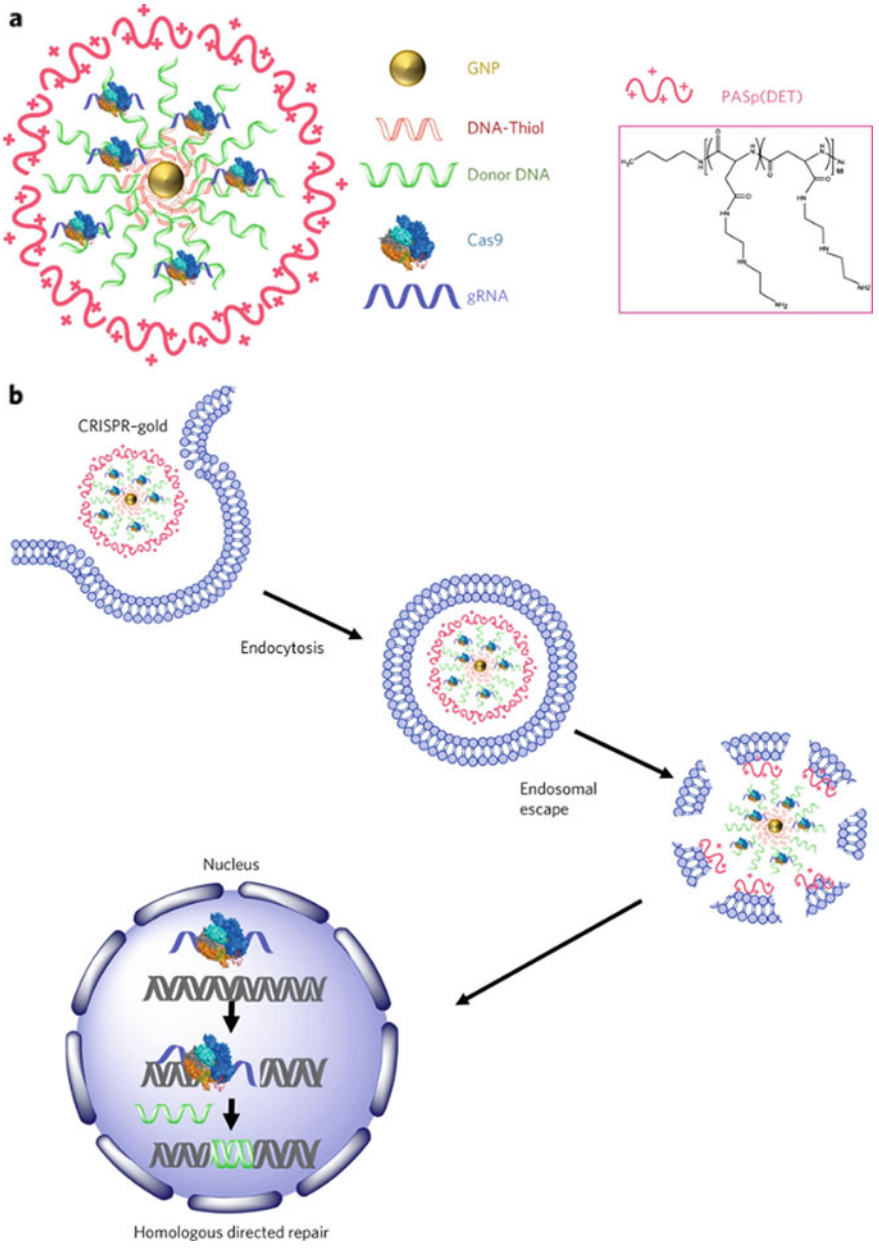

Fig. 4.7 **a** The components of CRISPR–Gold; **b** the working principle of CRISPR–Gold. Adapted with permission from Ref. [90]. Copyrights 2017 Springer Nature Limited

4.5 Conclusion and Future Perspective

This book chapter provides a summary of recent developments in the field of gold nanoparticles. Gold nanoparticles have been one of the most studied delivery systems because of their exciting physical, optical, chemical, and biological properties. Due to their biocompatibility, stability, and easy surface modifications, metal nanoparticles provide a promising platform for numerous biological applications, including the delivery of biomolecules, therapy, and diagnosis.

However, there are several critical issues that need to be addressed before their clinical applications. These issues may include the size and surface-dependent cytotoxicity, immune response, biodistribution, and targeting of a specific organ or tissue. These investigations will help design new delivery systems and enhance the understanding of nanomaterials' interaction with biological systems.

References

1. E.C. Dreaden, A.M. Alkilany, X. Huang, C.J. Murphy, M.A. El-Sayed, Chem. Soc. Rev. **41**, 2740 (2012)
2. R. Sardar, A.M. Funston, P. Mulvaney, R.W. Murray, Langmuir **25**, 13840 (2009)
3. J. Conde, J.T. Dias, V. GrazÃº, M. Moros, P.v. Baptista, J. M. de la Fuente, Front. Chem. **2** (2014)
4. P. Khandelwal, P. Poddar, J. Mater. Chem. B **5**, 9055 (2017)
5. S.S. Shankar, S. Bhargava, M. Sastry, J. Nanosci. Nanotech. **5**, 1721 (2005)
6. F. Kettemann, A. Birnbaum, S. Witte, M. Wuithschick, N. Pinna, R. Kraehnert, K. Rademann, J. Polte, Chem. Mater. **28**, 4072 (2016)
7. P.G. Jamkhande, N.W. Ghule, A.H. Bamer, M.G. Kalaskar, J. Drug Deliv. Sci. Technol. **53**, 101174 (2019)
8. C. Sharan, P. Khandelwal, P. Poddar, RSC Adv. **5**, 1883 (2015)
9. C. Sharan, P. Khandelwal, P. Poddar, RSC Adv. **5**, 91785 (2015)
10. P. Khandelwal, D.K. Singh, S. Sadhu, P. Poddar, Nanoscale **7**, 19985 (2015)
11. P. Khandelwal, D.K. Singh, S. Sadhu, P. Poddar, ChemPlusChem **79**, 134 (2014)
12. P. Khandelwal, A. Alam, A. Choksi, S. Chattopadhyay, P. Poddar, ACS Omega **3**, 4776 (2018)
13. D.K. Singh, R. Jagannathan, P. Khandelwal, P.M. Abraham, P. Poddar, Nanoscale **5**, 1882 (2013)
14. P.A. Pandey, G.R. Bell, J.P. Rourke, A.M. Sanchez, M.D. Elkin, B.J. Hickey, N.R. Wilson, Small **7**, 3202 (2011)
15. H. Nonomura, M. Nagata, H. Fujisawa, M. Shimizu, H. Niu, K. Honda, Appl. Phys. Lett. **86**, 163106 (2005)
16. T. Sugimoto, F. Shiba, T. Sekiguchi, H. Itoh, Colloids Surf. A Physicochem. Eng. Asp. **164**, 183 (2000)
17. T.S. Rodrigues, M. Zhao, T. Yang, K.D. Gilroy, A.G.M. da Silva, P.H.C. Camargo, Y. Xia, Chem. A Eur. J. **24**, 16944 (2018)
18. G. Su, C. Yang, J.-J. Zhu, Langmuir **31**, 817 (2015)
19. X. Ji, X. Song, J. Li, Y. Bai, W. Yang, X. Peng, J. Am. Chem. Soc. **129**, 13939 (2007)
20. J.D.S. Newman, G.J. Blanchard, Langmuir **22**, 5882 (2006)
21. Q. You, Y. Chen, J. Mater. Chem. C Mater. (2018)
22. D. Pan, J. Zhang, Z. Li, M. Wu, Adv. Mater. **22**, 734 (2010)
23. R.L. Penn, J.F. Banfield, Geochim. Cosmochim. Acta **63**, 1549 (1999)

24. Z. Liu, Y. Wang, Y. Zu, Y. Fu, N. Li, N. Guo, R. Liu, Y. Zhang, Mater. Sci. Eng. C **42**, 31 (2014)
25. N.-D. Tan, J.-H. Yin, Y. Yuan, L. Meng, N. Xu, Bull. Korean Chem. Soc. **1** (2018)
26. J. Liu, X. Ren, X. Meng, Z. Fang, F. Tang, Nanoscale **5**, 10022 (2013)
27. N. Xu, H. Li, Y. Wu, Anal. Chim. Acta **958**, 51 (2017)
28. J. Choi, S. Park, Z. Stojanović, H. Han, J. Lee, H.K. Seok, D. Uskoković, K.H. Lee, Langmuir **29**, 15698 (2013)
29. M. Carmen Bautista, O. Bomati-Miguel, M. del Puerto Morales, C. J. Serna, S. Veintemillas-Verdaguer, J. Mag. Mag. Mater. **293**, 20–27 (2005)
30. M. Gajbhiye, J. Kesharwani, A. Ingle, A. Gade, M. Rai, Nanomedicine **5**, 382 (2009)
31. Y. Zhou, Y. Yu, Y. Chai, R. Yuan, Talanta **181**, 32 (2018)
32. L. Shang, L. Yang, F. Stockmar, R. Popescu, V. Trouillet, M. Bruns, D. Gerthsen, G.U. Nienhaus, Nanoscale **4**, 4155 (2012)
33. K.-T. Chuang, Y.-W. Lin, J. Phys. Chem. C **121**, 26997 (2017)
34. Y. Liu, G.-F. Tian, X.-W. He, W.-Y. Li, Y.-K. Zhang, J. Mater. Chem. B **4**, 1276 (2016)
35. J.K.-J. Li, J. Med. Biol. Eng. **33**, 23 (2013)
36. F. Zhou, B. Feng, H. Yu, D. Wang, T. Wang, J. Liu, Q. Meng, S. Wang, P. Zhang, Z. Zhang, Y. Li, Theranostics **6**, 679 (2016)
37. T.C. Johnstone, K. Suntharalingam, S.J. Lippard, Chem. Rev. **116**, 3436 (2016)
38. X. Ling, J. Tu, J. Wang, A. Shajii, N. Kong, C. Feng, Y. Zhang, M. Yu, T. Xie, Z. Bharwani, B.M. Aljaeid, B. Shi, W. Tao, O.C. Farokhzad, ACS Nano Acsnano 8b06400 (2018)
39. Y. Shi, J. Goodisman, J.C. Dabrowiak, Inorg. Chem. **52**, 9418 (2013)
40. D. Pornpattananangkul, S. Olson, S. Aryal, M. Sartor, C. Huang, K. Vecchio, L. Zhang, ACS Nano **4**, 1935 (2010)
41. J. Li, X. Qu, G.F. Payne, C. Zhang, Y. Zhang, J. Li, J. Ren, H. Hong, C. Liu, Adv. Funct. Mater. **25**, 1404 (2015)
42. G. Liu, J. Li, D.-Q. Feng, J. Zhu, W. Wang, Anal. Chem. **89**, 1002 (2017)
43. H.S. El-Sawy, A.M. Al-Abd, T.A. Ahmed, K.M. El-Say, V.P. Torchilin, ACS Nano **12**, 10636 (2018)
44. F. Zhu, G. Tan, Y. Jiang, Z. Yu, F. Ren, Biomater Sci **6**, 2905 (2018)
45. X. Wang, X. Cai, J. Hu, N. Shao, F. Wang, Q. Zhang, J. Xiao, Y. Cheng, J. Am. Chem. Soc. **135**, 9805 (2013)
46. L. Qiu, Y. Zhao, N. Cao, L. Cao, L. Sun, X. Zou, Sens. Actuators B Chem. **234**, 21 (2016)
47. C.K. Kim, P. Ghosh, V.M. Rotello, Nanoscale **1** (2009)
48. C.W. Ng, J. Li, K. Pu, Adv. Funct. Mater. **28**, 1804688 (2018)
49. E.S. Shibu, M. Hamada, N. Murase, V. Biju, J. Photochem. Photobiol. C **15**, 53 (2013)
50. B.S. Dash, S. Das, J.-P. Chen, Int. J. Mol. Sci. **22**, 6658 (2021)
51. Z. Sun, L.-P. Zhang, F. Wu, Y. Zhao, Adv. Funct. Mater. **27**, 1704079 (2017)
52. A. Amendoeira, L.R. García, A.R. Fernandes, P.v. Baptista, Adv. Ther. (Weinh) **3**, 1900153 (2020)
53. L.v. Nair, S.S. Nazeer, R.S. Jayasree, A. Ajayaghosh, ACS Nano **9**, 5825 (2015)
54. S.S. Lucky, K.C. Soo, Y. Zhang, Chem. Rev. **115**, 1990 (2015)
55. S. Bhana, G. Lin, L. Wang, H. Starring, S.R. Mishra, G. Liu, X. Huang, ACS Appl. Mater. Interfaces **7**, 11637 (2015)
56. D. de Melo-Diogo, C. Pais-Silva, D.R. Dias, A.F. Moreira, I.J. Correia, Adv. Healthc. Mater. **6**, 1700073 (2017)
57. M.B.A. Nanocluster **102**, 2328 (2015)
58. W. Li, H. Zhang, X. Guo, Z. Wang, F. Kong, L. Luo, Q. Li, C. Zhu, J. Yang, Y. Lou, Y.-Z. Du, J. You, ACS Appl. Mater. Interfaces **9**, 3354 (2017)
59. M. Kim, J. Lee, J. Nam, Adv. Sci. **6**, 1900471 (2019)
60. L.C.W. Lin, S. Chattopadhyay, J.C. Lin, C.M.J. Hu, Adv. Healthc. Mater. **1701395**, 1 (2018)
61. S.T. Reddy, A.J. van der Vlies, E. Simeoni, V. Angeli, G.J. Randolph, C.P. O'Neil, L.K. Lee, M.A. Swartz, J.A. Hubbell, Nat. Biotechnol. **25**, 1159 (2007)

62. U. Sahin, P. Oehm, E. Derhovanessian, R.A. Jabulowsky, M. Vormehr, M. Gold, D. Maurus, D. Schwarck-Kokarakis, A.N. Kuhn, T. Omokoko, L.M. Kranz, M. Diken, S. Kreiter, H. Haas, S. Attig, R. Rae, K. Cuk, A. Kemmer-Brück, A. Breitkreuz, C. Tolliver, J. Caspar, J. Quinkhardt, L. Hebich, M. Stein, A. Hohberger, I. Vogler, I. Liebig, S. Renken, J. Sikorski, M. Leierer, V. Müller, H. Mitzel-Rink, M. Miederer, C. Huber, S. Grabbe, J. Utikal, A. Pinter, R. Kaufmann, J.C. Hassel, C. Loquai, Ö. Türeci, Nature **585**, 107 (2020)
63. A. Schudel, A.P. Chapman, M.K. Yau, C.J. Higginson, D.M. Francis, M.P. Manspeaker, A.R.C. Avecilla, N.A. Rohner, M.G. Finn, S.N. Thomas, Nat. Nanotechnol. **15**, 491 (2020)
64. C. Bourquin, D. Anz, K. Zwiorek, A.-L. Lanz, S. Fuchs, S. Weigel, C. Wurzenberger, P. von der Borch, M. Golic, S. Moder, G. Winter, C. Coester, S. Endres, J. Immunol. **181**, 2990 (2008)
65. L. Jeanbart, M. Ballester, A. de Titta, P. Corthesy, P. Romero, J.A. Hubbell, M.A. Swartz, Cancer Immunol. Res. **2**, 436 (2014)
66. S.N. Thomas, E. Vokali, A.W. Lund, J.A. Hubbell, M.A. Swartz, Biomaterials **35**, 814 (2014)
67. T. Fifis, A. Gamvrellis, B. Crimeen-Irwin, G.A. Pietersz, J. Li, P.L. Mottram, I.F.C. McKenzie, M. Plebanski, J. Immunol. **173**, 3148 (2004)
68. J.P.M. Almeida, E.R. Figueroa, R.A. Drezek, Nanomedicine **10**, 503 (2014)
69. I.H. Lee, H.K. Kwon, S. An, D. Kim, S. Kim, M.K. Yu, J.H. Lee, T.S. Lee, S.H. Im, S. Jon, Angewandte Chemie Int. Edn. **51**, 8800 (2012)
70. S. Ahn, I.H. Lee, S. Kang, D. Kim, M. Choi, P.E. Saw, E.C. Shin, S. Jon, Adv. Healthc. Mater. **3**, 1194 (2014)
71. K. Haume, S. Rosa, S. Grellet, M.A. Śmiałek, K.T. Butterworth, A.v. Solov'yov, K.M. Prise, J. Golding, N.J. Mason, Cancer Nanotechnol. **7**, 8 (2016)
72. D. Luo, A. Johnson, X. Wang, H. Li, B.O. Erokwu, S. Springer, J. Lou, G. Ramamurthy, C.A. Flask, C. Burda, T.J. Meade, J.P. Basilion, Nano Lett. **20**, 7159 (2020)
73. N. Goswami, Z. Luo, X. Yuan, D.T. Leong, J. Xie, Mater. Horiz. **4**, 817 (2017)
74. N. Ma, F. Wu, X. Zhang, Y. Jiang, H.-R. Jia, H. Wang, Y. Li, P. Liu, N. Gu, Z. Chen, ACS Appl. Mater. Interfaces **9**, 13037 (2017)
75. X. Fang, Y. Wang, X. Ma, Y. Li, Z. Zhang, Z. Xiao, L. Liu, X. Gao, J. Liu, J. Mater. Chem. B **5**, 4190 (2017)
76. J.F. Hainfeld, F.A. Dilmanian, D.N. Slatkin, H.M. Smilowitz, J. Pharm. Pharmacol. **60**, 977 (2010)
77. F. Ghahremani, D. Shahbazi-Gahrouei, A. Kefayat, H. Motaghi, M.A. Mehrgardi, S.H. Javanmard, RSC Adv. **8**, 4249 (2018)
78. Q. Chen, J. Chen, Z. Yang, J. Xu, L. Xu, C. Liang, X. Han, **1802228**, 1 (2019)
79. D. Huo, S. Liu, C. Zhang, J. He, Z. Zhou, H. Zhang, Y. Hu, ACS Nano **11**, 10159 (2017)
80. Y. Ding, Z. Sun, Z. Tong, S. Zhang, J. Min, Q. Xu, L. Zhou, Z. Mao, H. Xia, W. Wang, Theranostics **10**, 5195 (2020)
81. D.A. Giljohann, D.S. Seferos, A.E. Prigodich, P.C. Patel, C.A. Mirkin, J. Am. Chem. Soc. **131**, 2072 (2009)
82. A. Elbakry, A. Zaky, R. Liebl, R. Rachel, A. Goepferich, M. Breunig, Nano Lett. **9**, 2059 (2009)
83. I. Kaushik, S. Ramachandran, S.K. Srivastava, Semin. Cell Dev. Biol. **96**, 4 (2019)
84. M. Chen, A. Mao, M. Xu, Q. Weng, J. Mao, J. Ji, Cancer Lett. **447**, 48 (2019)
85. F.J. Sánchez-Rivera, T. Jacks, Nat. Rev. Cancer **15**, 387 (2015)
86. F.A. Ran, P.D. Hsu, J. Wright, V. Agarwala, D.A. Scott, F. Zhang, Nat. Protoc. **8**, 2281 (2013)
87. H. Nishimasu, X. Shi, S. Ishiguro, L. Gao, S. Hirano, S. Okazaki, T. Noda, O.O. Abudayyeh, J.S. Gootenberg, H. Mori, S. Oura, B. Holmes, M. Tanaka, M. Seki, H. Hirano, H. Aburatani, R. Ishitani, M. Ikawa, N. Yachie, F. Zhang, O. Nureki, Science (1979) **9129**, eaas9129 (2018)
88. C. Arnold, Nat. Med. **27**, 184 (2021)
89. H. Shivram, B.F. Cress, G.J. Knott, J.A. Doudna, Nat. Chem. Biol. **17**, 10 (2021)
90. K. Lee, M. Conboy, H.M. Park, F. Jiang, H.J. Kim, M.A. Dewitt, V.A. Mackley, K. Chang, A. Rao, C. Skinner, T. Shobha, M. Mehdipour, H. Liu, W.C. Huang, F. Lan, N.L. Bray, S. Li, J.E. Corn, K. Kataoka, J.A. Doudna, I. Conboy, N. Murthy, Nat. Biomed. Eng. **1**, 889 (2017)

91. Z. Glass, Y. Li, Q. Xu, Nat. Biomed. Eng. **1**, 854 (2017)
92. X. Tian, T. Gu, S. Patel, A.M. Bode, M.-H. Lee, Z. Dong, NPJ Precis. Oncol. **3**, 8 (2019)
93. F.A. Khan, N.S. Pandupuspitasari, H. Chun-Jie, Z. Ao, M. Jamal, A. Zohaib, F.A. Khan, M.R. Hakim, Z. ShuJun, Oncotarget **7**, 52541 (2016)
94. C. Jiang, X. Lin, Z. Zhao, Trends Mol. Med. **25**, 1039 (2019)
95. M.K. White, K. Khalili, Oncotarget **7**, 12305 (2016)
96. M. Martinez-Lage, P. Puig-Serra, P. Menendez, R. Torres-Ruiz, S. Rodriguez-Perales, Biomedicines **6**, 105 (2018)
97. S. Aghamiri, S. Talaei, A.A. Ghavidel, F. Zandsalimi, S. Masoumi, N.H. Hafshejani, V. Jajarmi, J. Drug Deliv. Sci. Technol. **56**, 101533 (2020)
98. F. Chen, M. Alphonse, Q. Liu, WIREs Nanomed. Nanobiotechnol. **12** (2020)
99. Y. Xu, R. Liu, Z. Dai, Nanoscale **12**, 21001 (2020)
100. B.E. Givens, Y.W. Naguib, S.M. Geary, E.J. Devor, A.K. Salem, AAPS J. **20**, 108 (2018)
101. P. Wang, L. Zhang, W. Zheng, L. Cong, Z. Guo, Y. Xie, L. Wang, R. Tang, Q. Feng, Y. Hamada, K. Gonda, Z. Hu, X. Wu, X. Jiang, Angew. Chem. **130**, 1507 (2018)